

Ba₂Gd₂(Si₄O₁₃): a silicate with finite Si₄O₁₃ chainsMaria Wierzbicka-Wieczorek,^{a*} Uwe Kolitsch^b and Ekkehart Tillmanns^a^aUniversität Wien, Institut für Mineralogie und Kristallographie, Geozentrum, Althanstrasse 14, A-1090 Wien, Austria, and ^bMineralogisch-Petrographische Abt., Naturhistorisches Museum Wien, Burgring 7, A-1010 Wien, Austria
Correspondence e-mail: maria.wierzbicka@univie.ac.at

Received 17 December 2009

Accepted 22 January 2010

Online 3 February 2010

The title compound, dibarium digadolinium(III) tetrasilicate, crystallized from a molybdate-based flux. It represents a new structure type and contains finite zigzag-shaped C_2 -symmetric Si₄O₁₃ chains and Gd₂O₁₂ dimers built of edge-sharing GdO₇ polyhedra. The [9+1]-coordinated Ba atoms are located in voids in the atomic arrangement. All atoms are in general positions except for one O atom, which lies on a twofold axis. The structure is compared with those of the few other known tetrasilicates.

Comment

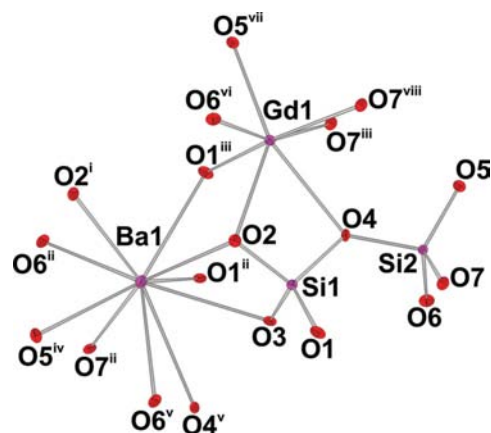
In a comprehensive ongoing study we are focusing on the preparation, structural characterization and classification of novel microporous and small-pore mixed-framework silicates containing seven specific octahedrally coordinated M^{3+} cations ($M = \text{Sc, V, Cr, Fe, In, Y}$ and Yb). These poorly known members of the silicate family are expected to have useful properties and interesting technical applications, similar to the related mixed-framework (SiO₄- M^{4+} O₆) titanosilicates and zirconosilicates. As part of our study, we have recently also included compounds containing the Gd³⁺ cation for comparison purposes, as this cation may either show octahedral coordination or have higher coordination numbers (7–8). The title compound, (I), was obtained as a by-product during the preparation of the Gd analogue of BaY₂Si₃O₁₀ and isotypic Sc and lanthanide representatives (Kolitsch *et al.*, 2006; Wierzbicka-Wieczorek, 2007; see also Kolitsch *et al.*, 2009). It represents a novel structure type and is a new representative of a small class of tetrasilicates with finite Si₄O₁₃ chains (groups).

Additional flux-growth syntheses involving Gd³⁺ have so far yielded the following three Gd silicates: Rb₃GdSi₈O₁₉ and Cs₃GdSi₈O₁₉, both isotypic with Cs₃ScSi₈O₁₉ (Kolitsch & Tillmanns, 2004), and BaKGdSi₂O₇, isotypic with the disilicates BaKREESi₂O₇ (REE = Y, Yb and Sc; Kolitsch *et al.*, 2009) and SrKScSi₂O₇ (Wierzbicka-Wieczorek, 2007).

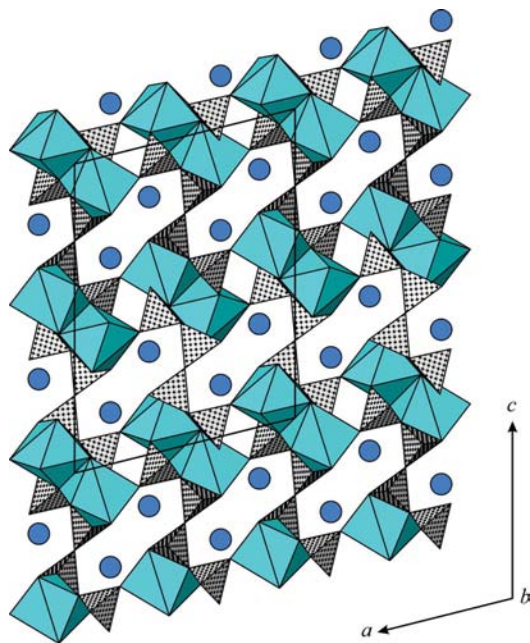
The asymmetric unit in monoclinic (I) contains one Ba, one Gd, two Si and seven O atoms (Fig. 1). All atoms are in general positions except O3, which lies on a twofold axis. Bond-valence sums for all atoms were calculated using the bond-valence parameters from Brese & O'Keeffe (1991): 2.01 (Ba), 3.05 (Gd), 3.99 (Si1), 3.85 (Si2), 2.06 (O1), 2.08 (O2), 2.27 (O3), 1.94 (O4), 1.84 (O5), 1.86 (O6) and 1.96 (O7) v.u. (valence units). Thus, these are all reasonably close to ideal valencies. (The oxygen ligands O3 and O4 represent bridging O atoms within the finite Si₄O₁₃ chain and are expected to have slightly high bond-valence sums. However, only atom O3 shows an elevated value, while O4, bonded also to Gd, shows a normal value.)

The atomic arrangement is based on finite zigzag-shaped Si₄O₁₃ chains and Gd₂O₁₂ dimers built of edge-sharing GdO₇ polyhedra (Fig. 2). The latter are rather irregular, although they may be described as monocapped octahedra (the capping atom being O6). The Gd₂O₁₂ dimers are linked by SiO₄ tetrahedra to form a heteropolyhedral slab in the *ab* plane. These slabs are connected to adjacent slabs only *via* a bridging O3 atom of the Si₄O₁₃ chain. The SiO₄ tetrahedron shares the O2–O4 edge with the GdO₇ polyhedron. The [9+1]-coordinated Ba atoms are located in voids of the atomic arrangement, with Ba–O distances in the range 2.699 (3)–3.319 (3) Å.

The two non-equivalent SiO₄ tetrahedra form a tetrasilicate group (Si₄O₁₃) which can also be described as a finite chain. The bond-length distortion of the SiO₄ tetrahedra is remarkable (Table 1) and more pronounced than in comparable di- and trisilicates. The bond-angle distortion is also very strong; for the Si1O₄ and Si2O₄ tetrahedra the distortion parameters $\sigma(\text{oct})^2$ (Robinson *et al.*, 1971) are 38.60 and 22.09, respectively. The most distorted SiO₄ units are the two Si1-centred ones in the centre of the finite chain. This can be explained by the electrostatic repulsion between Si1 and the neighbouring Si1 and Si2 atoms. A similarly strong distortion of SiO₄

**Figure 1**

A view of the basic connectivity in Ba₂Gd₂(Si₄O₁₃), shown with displacement ellipsoids at the 50% probability level. [Symmetry codes: (i) $-x + \frac{1}{2}, y + \frac{1}{2}, -z + \frac{1}{2}$; (ii) $-x, y + 1, -z + \frac{1}{2}$; (iii) $x, y + 1, z$; (iv) $x + \frac{1}{2}, -y + \frac{1}{2}, z + \frac{1}{2}$; (v) $-x, y, -z + \frac{1}{2}$; (vi) $x + \frac{1}{2}, y + \frac{1}{2}, z$; (vii) $-x, -y + 1, -z$; (viii) $-x, -y, -z$.]

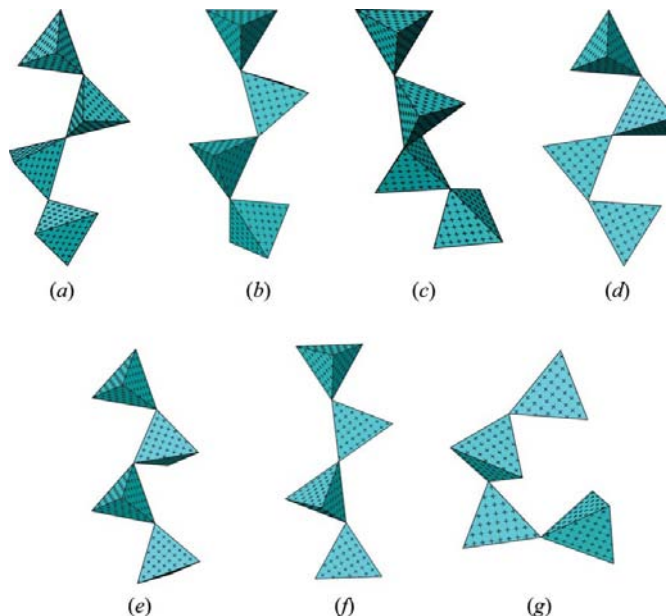

Figure 2

A view of $\text{Ba}_2\text{Gd}_2(\text{Si}_4\text{O}_{13})$ along [010]. Dimers built of edge-sharing GdO_7 polyhedra are linked *via* a zigzag-shaped finite Si_4O_{13} chain (SiO_4 tetrahedra are marked with crosses). Ba atoms are shown as spheres. The unit cell is outlined.

tetrahedra is observed in other chemically related tetrasilicates such as $\text{Ba}_2\text{Nd}_2(\text{Si}_4\text{O}_{13})$ (range of Si—O bond lengths in the most distorted SiO_4 unit is 1.582–1.670 Å; Tamazyan & Malinovskii, 1985).

The configuration of the finite C_2 -symmetric tetrasilicate group (Si_4O_{13}) in (I) has a zigzag shape, with Si··Si··Si angles of $99.88(5)^\circ$ (Table 1). The chain configuration in (I) may be compared with those in the few other tetrasilicates reported so far (Fig. 3). The first of these was only described in 1979 [$\text{Ag}_{10}(\text{Si}_4\text{O}_{13})$; Jansen & Keller, 1979]. The Si_4O_{13} unit in this compound is zigzag-shaped as well (Fig. 3*b*). A similar zigzag configuration is also shown by $\text{Na}_4\text{Sc}_2(\text{Si}_4\text{O}_{13})$ (Maksimov *et al.*, 1980; Fig. 3*c*), $\text{Ba}_2\text{Nd}_2(\text{Si}_4\text{O}_{13})$ (Tamazyan & Malinovskii, 1985; Fig. 3*d*) and $\text{K}_5\text{Eu}_2\text{F}(\text{Si}_4\text{O}_{13})$ (Chiang *et al.*, 2007; Fig. 3*e*). Two further reported tetrasilicates contain Si_4O_{13} units but also additional silicate groups. Both $\text{Ag}_{18}(\text{SiO}_4)_2(\text{Si}_4\text{O}_{13})$ (Heidebrecht & Jansen, 1991*a,b*) and $\text{La}_6(\text{Si}_4\text{O}_{13})(\text{SiO}_4)_2$ (Müller-Bunz & Schleid, 2002; I-type modification of $\text{La}_2\text{Si}_2\text{O}_7$) contain isolated SiO_4 groups. The Ag silicate is characterized by an Si_4O_{13} unit with a stretched zigzag configuration (Fig. 3*f*). The La silicate has an unusual horseshoe-shaped Si_4O_{13} unit (Fig. 3*g*), probably because of the additional presence of two isolated SiO_4 tetrahedra.

Fig. 3 clearly demonstrates that the configuration in (I) (Fig. 3*a*) is most similar to that in $\text{Ag}_{10}(\text{Si}_4\text{O}_{13})$ (Fig. 3*b*) and least similar to those in $\text{La}_6(\text{Si}_4\text{O}_{13})(\text{SiO}_4)_2$ (Fig. 3*g*; horseshoe-shaped unit) and $\text{Na}_4\text{Sc}_2\text{Si}_4\text{O}_{13}$ (Fig. 3*c*; twisted unit). This similarity is also reflected in the Si··Si··Si angles in these silicates: the angle in (I), $99.88(5)^\circ (\times 2)$, is fairly similar to the Si··Si··Si angles in $\text{Ag}_{10}(\text{Si}_4\text{O}_{13})$ (101.0 and 110.2°) and


Figure 3

An overview of the configurations of the Si_4O_{13} unit in the known tetrasilicates. (a) $\text{Ba}_2\text{Gd}_2(\text{Si}_4\text{O}_{13})$, (b) $\text{Ag}_{10}(\text{Si}_4\text{O}_{13})$, (c) $\text{Na}_4\text{Sc}_2(\text{Si}_4\text{O}_{13})$, (d) $\text{Ba}_2\text{Nd}_2(\text{Si}_4\text{O}_{13})$, (e) $\text{K}_5\text{Eu}_2\text{F}(\text{Si}_4\text{O}_{13})$, (f) $\text{Ag}_{18}(\text{SiO}_4)_2(\text{Si}_4\text{O}_{13})$ and (g) $\text{La}_6(\text{Si}_4\text{O}_{13})(\text{SiO}_4)_2$.

$\text{K}_5\text{Eu}_2\text{F}(\text{Si}_4\text{O}_{13})$ (102.8 and 104.3°), whereas the values in $\text{Ba}_2\text{Nd}_2(\text{Si}_4\text{O}_{13})$ are distinctly smaller (85.1 and 85.3°), and those in $\text{Na}_4\text{Sc}_2(\text{Si}_4\text{O}_{13})$ (125.7 and 126.0°) and $\text{Ag}_{18}(\text{SiO}_4)_2(\text{Si}_4\text{O}_{13})$ ($2 \times 125.9^\circ$) are distinctly larger. The unusual horseshoe-shaped unit in $\text{La}_6(\text{Si}_4\text{O}_{13})(\text{SiO}_4)_2$ shows fairly small Si··Si··Si angles, 91.0 and 100.7° . The cation radii of the non-Si cations in these silicates appear to be negatively correlated with the Si··Si··Si angle: the silicate with the largest cations [$\text{Ba}_2\text{Nd}_2(\text{Si}_4\text{O}_{13})$] is characterized by the smallest Si··Si··Si angles, whereas the silicate with the smallest cations [$\text{Na}_4\text{Sc}_2(\text{Si}_4\text{O}_{13})$] exhibits the largest Si··Si··Si angles. Compound (I) and $\text{K}_5\text{Eu}_2\text{F}(\text{Si}_4\text{O}_{13})$ show an intermediate behaviour.

The connectivities in the crystal structures of $\text{Na}_4\text{Sc}_2(\text{Si}_4\text{O}_{13})$, $\text{K}_5\text{Eu}_2\text{F}(\text{Si}_4\text{O}_{13})$ and $\text{Ba}_2\text{Nd}_2(\text{Si}_4\text{O}_{13})$ are slightly similar to that in (I). The first silicate contains Sc_2O_{10} dimers (composed of two ScO_6 octahedra sharing one common edge), comparable with the Gd_2O_{12} dimers in (I). In contrast with (I), no edge is shared between an Sc-centred polyhedron and an SiO_4 tetrahedron. $\text{K}_5\text{Eu}_2\text{F}(\text{Si}_4\text{O}_{13})$ contains $\text{Eu}_2\text{O}_{10}\text{F}$ dimers composed of two corner-sharing EuO_5F octahedra (the F atom is the shared atom). In $\text{Ba}_2\text{Nd}_2(\text{Si}_4\text{O}_{13})$, NdO_8 polyhedra are edge-linked to each other, thereby forming an incomplete polyhedral layer parallel to (011). Despite the strong similarity of the respective chain units, the connectivity in $\text{Ag}_{10}(\text{Si}_4\text{O}_{13})$ bears no similarity to that in (I), and this is most likely due to the irregular coordination environments of the Ag atoms and a much higher metal:Si ratio.

Although the structural formula of the complex silicate $\text{NaBa}_3\text{Nd}_3(\text{Si}_2\text{O}_7)(\text{Si}_4\text{O}_{13})$ (Malinovskii *et al.*, 1983) again suggests that this compound also contains finite chains, the

Si₄O₁₃ unit is in fact a branched finite Si₃O₁₀ chain (insular tetramer). The finite chain anion (Si₄O₁₃)¹⁰⁻ has not only been found in silicates, but also in acid aqueous solutions during the trimethylsilylation of Ag₁₀(Si₄O₁₃) (Calhoun *et al.*, 1980).

Interestingly, tetrasilicates containing finite Si₄O₁₃ chains have not been reported yet in nature. Furthermore, only one germanate is known that contains finite Ge₄O₁₃ chains, namely Cu₂Fe₂(Ge₄O₁₃) (Masuda *et al.*, 2003); it is characterized by a slightly curved chain (with all GeO₄ tetrahedra in an eclipsed orientation), a geometry completely different from those of the above silicates. A larger number of phosphates with finite P₄O₁₃ chains are known (see references cited in Alekseev *et al.*, 2009), but only a single arsenate with a finite As₄O₁₃ chain was described very recently {Ag₆[(UO₂)₂(As₂O₇)(As₄O₁₃)], with a zigzag configuration of the As₄O₁₃ unit; Alekseev *et al.*, 2009}. Among vanadates, there are only three known examples containing finite V₄O₁₃ chains. All of these are characterized by a horseshoe-shaped configuration {Ba₃[V₄O₁₃] (Gatehouse *et al.*, 1987), Fe₂[V₄O₁₃] (Permer & Lligant, 1997) and {[NH₃(CH₂)₃NH₂]Zn³⁺[V₄O₁₃]⁶⁻ (Natarajan, 2003)}. If chromates are considered, one finds again a larger number of examples, such as K₂[Cr₄O₁₃] (Casari & Langer, 2005) and Cs₂[Cr₄O₁₃] (Kolitsch, 2004), all with a zigzag configuration.

Experimental

The title compound was crystallized from a BaO–Rb₂O–MoO₃ flux containing dissolved precursor compounds of Ba, Rb, Gd and Si. The experimental parameters were: BaCO₃ (1.0022 g), Rb₂CO₃ (0.5997 g), MoO₃ (1.0020 g), Gd₂O₃ (0.1727 g) and SiO₂ (0.1611 g); Pt crucible covered with a lid, T_{\max} = 1423 K, holding time = 3 h, cooling rate = 2 K h⁻¹, T_{\min} = 1173 K, slow cooling to room temperature after switching off the furnace. The reaction products were recovered by dissolving the Rb–molybdate flux solvent in distilled water. Ba₂Gd₂(Si₄O₁₃) formed small colourless pseudotetragonal prisms, which were accompanied by tiny prisms of BaY₂Si₃O₁₀ type (Kolitsch *et al.*, 2006) and BaREE³⁺Si₃O₁₀ (REE = Gd, Er, Yb and Sc; Wierzbicka-Wieczorek, 2007).

Crystal data

Ba ₂ Gd ₂ (Si ₄ O ₁₃)	$V = 1144.1 (5) \text{ \AA}^3$
$M_r = 909.52$	$Z = 4$
Monoclinic, $C2/c$	Mo $K\alpha$ radiation
$a = 12.896 (3) \text{ \AA}$	$\mu = 18.73 \text{ mm}^{-1}$
$b = 5.212 (1) \text{ \AA}$	$T = 293 \text{ K}$
$c = 17.549 (4) \text{ \AA}$	$0.08 \times 0.08 \times 0.02 \text{ mm}$
$\beta = 104.08 (3)^\circ$	

Data collection

Bruker APEXII CCD area-detector diffractometer	11887 measured reflections
Absorption correction: multi-scan (SADABS; Bruker, 2006)	2625 independent reflections
$T_{\min} = 0.316$, $T_{\max} = 0.706$	1910 reflections with $I > 2\sigma(I)$
	$R_{\text{int}} = 0.032$

Refinement

$R[F^2 > 2\sigma(F^2)] = 0.026$	97 parameters
$wR(F^2) = 0.046$	$\Delta\rho_{\max} = 1.30 \text{ e \AA}^{-3}$
$S = 1.04$	$\Delta\rho_{\min} = -1.65 \text{ e \AA}^{-3}$
2625 reflections	

Table 1

Selected geometric parameters (\AA , $^\circ$).

Ba1—O ² _i	2.669 (3)	Gd1—O ¹ _{iii}	2.331 (3)
Ba1—O ⁶ _{ii}	2.710 (3)	Gd1—O ²	2.382 (3)
Ba1—O ¹ _{iii}	2.802 (3)	Gd1—O ⁷ _{iii}	2.485 (3)
Ba1—O ²	2.827 (3)	Gd1—O ⁴	2.625 (3)
Ba1—O ⁵ _{iv}	2.841 (3)	Si1—O ¹	1.589 (3)
Ba1—O ³	2.890 (2)	Si1—O ²	1.602 (3)
Ba1—O ⁷ _{ii}	2.947 (3)	Si1—O ³	1.6481 (15)
Ba1—O ⁴ _v	3.041 (3)	Si1—O ⁴	1.667 (3)
Ba1—O ⁶ _v	3.055 (3)	Si2—O ⁵	1.595 (3)
Ba1—O ¹ _{ii}	3.319 (3)	Si2—O ⁶	1.625 (3)
Gd1—O ⁶ _{vi}	2.294 (3)	Si2—O ⁷	1.646 (3)
Gd1—O ⁵ _{vii}	2.299 (3)	Si2—O ⁴	1.692 (3)
Gd1—O ⁷ _{viii}	2.302 (3)		
Si1 ^v —O ³ —Si1	143.2 (2)	Si2—Si1—Si1 ^v	99.88 (5)
Si1—O ⁴ —Si2	125.18 (16)		

Symmetry codes: (i) $-x + \frac{1}{2}, y + \frac{1}{2}, -z + \frac{1}{2}$; (ii) $-x, y + 1, -z + \frac{1}{2}$; (iii) $x, y + 1, z$; (iv) $x + \frac{1}{2}, -y + \frac{1}{2}, z + \frac{1}{2}$; (v) $-x, y, -z + \frac{1}{2}$; (vi) $x + \frac{1}{2}, y + \frac{1}{2}, z$; (vii) $-x, -y + 1, -z$; (viii) $-x, -y, -z$.

The highest residual electron-density peak is 0.75 \AA from the Gd1 site and the deepest hole is 1.24 \AA from the Ba1 site.

Data collection: APEX2 (Bruker, 2008); cell refinement: SAINT (Bruker, 2008); data reduction: SAINT; program(s) used to solve structure: SHELXS97 (Sheldrick, 2008); program(s) used to refine structure: SHELXL97 (Sheldrick, 2008); molecular graphics: ATOMS (Shape Software, 1999); software used to prepare material for publication: SHELXL97.

Financial support from the Austrian Science Foundation (FWF) (grant No. P15220-N06) is gratefully acknowledged.

Supplementary data for this paper are available from the IUCr electronic archives (Reference: LG3027). Services for accessing these data are described at the back of the journal.

References

- Alekseev, E. V., Krivovichev, S. V. & Depmeier, W. (2009). *J. Mater. Chem.* **19**, 2583–2587.
- Brese, N. E. & O'Keeffe, M. (1991). *Acta Cryst.* **B47**, 192–197.
- Bruker (2006). SADABS. Bruker AXS Inc., Madison, Wisconsin, USA.
- Bruker (2008). APEX2 and SAINT. Bruker AXS Inc., Madison, Wisconsin, USA.
- Calhoun, H. P., Masson, C. R. & Jansen, M. (1980). *J. Chem. Soc. Chem. Commun.* pp. 576–577.
- Casari, B. M. & Langer, V. (2005). *Acta Cryst.* **C61**, i117–i119.
- Chiang, P.-Y., Lin, T.-W., Dai, J.-H., Chang, B.-C. & Lii, K.-H. (2007). *Inorg. Chem.* **46**, 3619–3622.
- Gatehouse, B. M., Guddat, L. W. & Roth, R. S. (1987). *J. Solid State Chem.* **71**, 390–395.
- Heidebrecht, K. & Jansen, M. (1991a). *Z. Anorg. Allg. Chem.* **597**, 79–86.
- Heidebrecht, K. & Jansen, M. (1991b). *Z. Anorg. Allg. Chem.* **606**, 242.
- Jansen, M. & Keller, H. L. (1979). *Angew. Chem.* **91**, 500.
- Kolitsch, U. (2004). *Acta Cryst.* **C60**, i17–i19.
- Kolitsch, U. & Tillmanns, E. (2004). *Mineral. Mag.* **68**, 677–686.
- Kolitsch, U., Wierzbicka, M. & Tillmanns, E. (2006). *Acta Cryst.* **C62**, i97–i99.
- Kolitsch, U., Wierzbicka-Wieczorek, M. & Tillmanns, E. (2009). *Can. Mineral.* **47**, 421–431.
- Maksimov, B. A., Mel'nikov, O. K., Zhdanova, T. A. & Ilyukhin, V. V. (1980). *Dokl. Akad. Nauk SSSR*, **251**, 98–102.
- Malinovskii, Yu. A., Baturin, S. V. & Bondareva, O. S. (1983). *Dokl. Akad. Nauk SSSR*, **272**, 865–869.
- Masuda, T., Chakoumakos, B. C., Nygren, C. L., Imai, S. & Uchinokura, K. (2003). *J. Solid State Chem.* **176**, 175–179.

- Müller-Bunz, H. & Schleid, T. (2002). *Z. Anorg. Allg. Chem.* **628**, 564–569.
- Natarajan, S. (2003). *Inorg. Chim. Acta*, **348**, 233–236.
- Permer, L. & Laligant, Y. (1997). *Eur. J. Solid State Inorg. Chem.* **34**, 41–52.
- Robinson, K., Gibbs, G. V. & Ribbe, P. H. (1971). *Science*, **172**, 567–570.
- Shape Software (1999). *ATOMS for Windows and Macintosh*. Version 5.0.4. Shape Software, Kingsport, Tennessee, USA.
- Sheldrick, G. M. (2008). *Acta Cryst.* **A64**, 112–122.
- Tamazyan, R. A. & Malinovskii, Yu. A. (1985). *Dokl. Akad. Nauk SSSR*, **285**, 124–183.
- Wierzbicka-Wieczorek, M. (2007). PhD thesis, University of Vienna, Austria.